Nanosecond Dynamics of Single Polypeptide Molecules Revealed by Photoemission Statistics of Fluorescence Resonance Energy Transfer: A Theoretical Study

Zhisong Wang* and Dmitrii E. Makarov*

Department of Chemistry and Biochemistry and Institute for Theoretical Chemistry, University of Texas at Austin, Austin, Texas 78712

Received: February 3, 2003; In Final Form: April 15, 2003

Recently single molecule photoemission statistics have been measured with a nanosecond time resolution for a pair of dye molecules attached to a DNA molecule and undergoing fluorescence resonance energy transfer (FRET) [Berglund, A. J.; Doherty, A. C.; Mabuchi, H. *Phys. Rev. Lett.* **2002**, *89*, 068101]. We have simulated single molecule photoemission in a model, where a FRET pair resides on a polypeptide molecule that undergoes diffusion in water, with the goal to understand how the dynamics of the molecule are reflected in the observed photoemission statistics. We further compare our simulation results with the classical theory of Haas and Steinberg [Haas, E.; Steinberg, I. Z. *Biophys. J.* **1984**, *46*, 429] and find that their approximation, while not quantitative in the case of fast diffusion in water, predicts well many of the qualitative features of the single molecule photoemission signal. The calculated second-order intensity autocorrelation functions exhibit photon antibunching at short times and photon bunching at longer times, the latter being crucially dependent on the time scales of intramolecular diffusion as well as on the properties of the FRET pair. Our study establishes potentially useful guidelines for the choice of FRET pairs for the experimental study of specific systems.

1. Introduction

Single molecule fluorescence resonance energy transfer (FRET) is an increasingly popular method of probing the complex dynamics of biomolecules.[1−7] In a typical FRET experiment, one uses a pair of chromophores planted on a molecule of interest. When one of them, the donor (D), is excited by a laser, the excitation energy can be transferred to the other one, the acceptor (A), provided that the emission spectrum of the donor overlaps with the absorption spectrum of the acceptor. The fluorescence signal from the acceptor then depends on the FRET rate

$$\Gamma_F = \frac{1}{\tau_D}\left(\frac{R_0}{r}\right)^6 \tag{1}$$

where R_0 is the Förster radius, τ_D is the donor emission lifetime, and r the distance between the donor and the acceptor. The FRET rate is thus very sensitive to r providing a "spectroscopic ruler" that allows one to measure the dimensions of the probed molecule.

Until recently, most single molecule FRET studies focused on the fluctuations of the FRET efficiency $E(t) = \Gamma_F(t)/(\Gamma_F(t) + 1/\tau_D)$, which are related to the fluctuations of the distance $r(t)$. From such measurements, probability distributions for r and thus effective free energy surfaces $G(r)$ have been inferred.[2−5] The interpretation of such experiments is however confounded by their finite time resolution:[4] If the molecule reconfigures on a time scale that is faster than that of the measurement, then information about these fast fluctuations (and the associated probability distribution of the distance $p(r)$) is lost; instead one observes an effective averaged value of r. FRET studies with improved time resolution are also desirable if one wishes to probe the dynamics of conformational changes that occur in the molecule and are reflected in the fluctuations of $r(t)$.

Recently, Berglund and co-workers[8] reported nanosecond time-resolution measurements of photon statistics from a pair of dye molecules attached to a DNA molecule. In addition to the photon antibunching that is due to the quantum mechanical nature of the emitted light, they have observed photon bunching at a longer time scale: The latter reflects the internal dynamics of the chromophores and/or the probed molecule. This approach thus has the capability of probing fast dynamical processes occurring in molecules at a nanosecond time scale. Such processes may, for example, include the formation of secondary structure and large conformational rearrangements in proteins.[9] In addition, because of their better time resolution, these measurements may avoid the above self-averaging problem and provide a way to probe the equilibrium distance distributions $p(r)$ for interchromophore distances thus potentially leading to accurate measurements of proteins' free energy landscapes.

To better understand what kind of information can be extracted from such measurements, in this paper, we simulate a single-molecule FRET experiment, in which two dye molecules are attached to the ends of a denatured polypeptide chain. The main question we intend to address is the relationship between the observed intensity correlation functions for the photons emitted by a single FRET pair and the dynamics of the chain. This question has previously been addressed in the pioneering study of Haas and Steinberg,[10] who, in particular, showed that diffusive dynamics of the distance between the donor and the acceptor may lead to a bunching signal in the donor emission intensity autocorrelation function, allowing a measurement of the intramolecular diffusion coefficient. Also Yang and co-workers have recently studied the statistical properties of the FRET efficiency and of the FRET lifetime for semiflexible Gaussian chains.[11]

These classical theories imply that the chromophore dynamics are slow compared to the photoemission rate, and accordingly,

* To whom correspondence should be addressed. E-mail: zswang@mail.cm.utexas.edu or makarov@mail.cm.utexas.edu.

10.1021/jp034285o CCC: $25.00
Published on Web 05/20/2003

they do not take into account the quantum nature of the single molecule radiation. However, if an experiment of the kind reported in ref 8 is performed on a single protein molecule in water, this assumption will likely be violated. Indeed, suppose the relative motion of the two ends of the chain is characterized by an intramolecular diffusion coefficient typical of protein molecules in water,[9,12−14] $D \sim 10^{-6}-10^{-5}$ cm^2/s, and that the Förster radius for the pair of dye molecules attached at the ends of the chain is $R_0 \sim 20$ Å. The time it takes the pair to diffuse over a distance $\sim R_0$ thereby considerably changing the emission signal is $t \sim R_0^2/D \sim 4-40$ ns. This time is comparable to a typical emission time τ_D, which is normally in a nanosecond range. Thus, the distance between the chromophores may change considerably during the time between two subsequent photon emission events. This leads to a nontrivial interplay between the time scales of photon emission, intramolecular diffusion, and FRET and calls for a study that takes into account the quantum nature of the emitted light and treats all of these time scales on the same footing, which is undertaken in the present paper. The relationships between single-molecule dynamics and photoemission statistics have previously been studied in different contexts.[15−18]

This paper is organized as follows: In section II, we describe our model, and in section III, we report our results. In sections IV and V, we compare our simulation results with the Haas−Steinberg theory[10] and with the dynamics of the dual FRET model introduced in.[8] Section VI concludes with closing remarks.

II. The Model

Dynamics of the Polypeptide Chain in Solution. We use a Monte Carlo procedure to generate an ensemble of random polyalanine chains satisfying appropriate excluded volume constraints. The details of our approach can be found in refs 12 and 19. This procedure allows us to generate the equilibrium distribution $p(\mathbf{r})$ for the distance $\mathbf{r}$ between the chromophores. We also note that it is possible to directly extract $p(\mathbf{r})$ from experimental data.[10,20] In our model, we make the simplifying assumption that the chromophores are attached at the ends of the chain and that $\mathbf{r}$ is simply the distance between its outermost side chains. We then assume[12,20,21] that the relative motion of the chain ends can be described as diffusion in an effective potential $G(\mathbf{r})$ defined as

$$\exp(-G(\mathbf{r})/k_B T) = p(\mathbf{r})$$

with a diffusion coefficient D. To generate trajectories $\mathbf{r}(t)$ of this motion, we perform Brownian dynamics simulation using the velocity Verlet algorithm.[22] The instantaneous value of the distance $\mathbf{r}(t)$ determines, at each moment, the probability of excitation transfer from the donor (D) to the acceptor (A), according to eq 1.

In Figure 1, we show the probability distribution for the dye separation, $p(\mathbf{r})$, for a chain that consists of 23 peptide units. The peptide bonds confine the chain ends within 60 Å from each other, while bending rigidity and the excluded volume effect prevent the ends from being too close to one another ($r > 5$Å). As a consistency check, shown in Figure 1 are both the original probability distribution $p(\mathbf{r})$ generated by Monte Carlo and the distribution generated by the Brownian dynamics algorithm; Naturally, the two are the same to within statistical errors.

FRET Dynamics. The energy level diagram of the two chromophores is shown in Figure 2. We assume that the donor

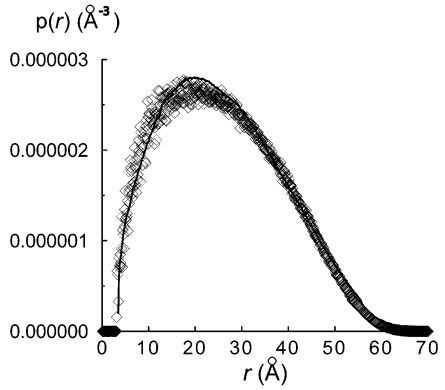

Figure 1. Probability distribution for the end-end distance of a polyalanine chain consisting of 23 peptide units. The solid line is Monte Carlo sampling, the diamonds are Brownian dynamics simulation.

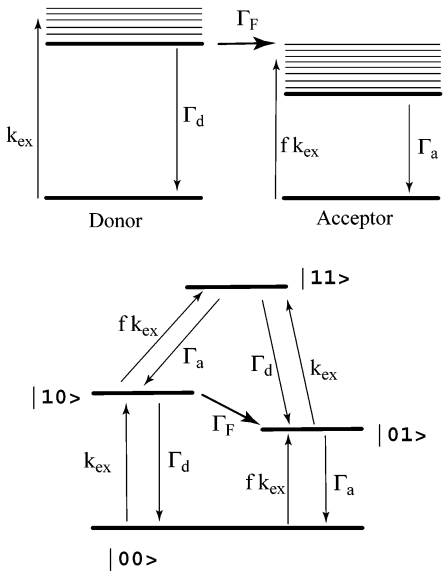

Figure 2. (a) Energy levels of the donor and acceptor. (b) Electronic states and the transitions included in the present model.

excitation is incoherent and is described by an excitation rate k_{ex}. The acceptor can also become excited by the laser albeit with a smaller rate, fk_{ex}, where $f < 1$. The donor and acceptor emission lifetimes are $\tau_D = 1/\Gamma_d$ and $1/\Gamma_a$, respectively, and the FRET rate $\Gamma_F = \Gamma_F(\mathbf{r}(t))$ depends on time according to eq 1. The electronic states of the FRET pair include the ground state $|00\rangle$, the state in which only the donor or only the acceptor is excited, ($|10\rangle$ and $|01\rangle$, respectively) and the state $|11\rangle$ where both the donor and the acceptor are excited (Figure 2b). The population of each of these states is governed by the equations

$$d\rho_{ii}/dt = \sum_j k_{ji}(t)\rho_{jj} - \sum_j k_{ij}(t)\rho_{ii} \qquad (2)$$

where ρ stands for the density matrix of the system, the subscripts i and j label the four electronic states of the system shown in Figure 2b and k_{ij} is the transition rate from state i to state j. For example, for i and j corresponding to $|11\rangle$ and $|10\rangle$, the rate k_{ij} is equal to Γ_a, and for the transition from $|10\rangle$ to $|01\rangle$, we have $k_{ij} = \Gamma_F(\mathbf{r}(t))$.

Because we are interested in the photoemission statistics, instead of solving the equations (2) directly, we apply a stochastic algorithm that simulates the evolution of the FRET pair as they undergo jumps among the four available states. The Monte Carlo wave function approach[23−28] is well suited for this kind of simulations. However, because in this particular

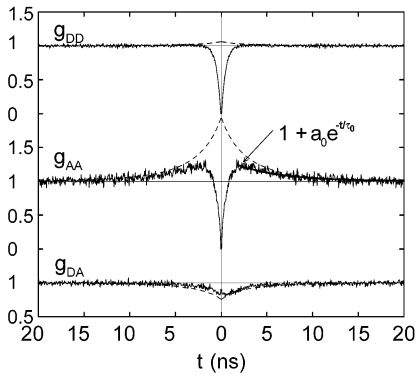

Figure 3. Second-order intensity correlation functions for the FRET pair attached to a peptide that consists of 23 units. The intramolecular diffusion coefficient is $D = 3 \times 10^{-6}$ cm^2/s and the Förster radius is $R_0 = 20$ Å. The solid lines are the simulation results, and the dashed lines are the predictions of eq 6.

case coherences are unimportant, eq 2 is effectively a classical rate equation and the same result is obtained by using the classical kinetic Monte Carlo algorithm.[29,30] In this algorithm, stochastic "trajectories" of the system are generated according to the probabilities determined by eq 2. Specifically, if the system is found in state i at some time t, then, during a short time interval Δt, it can undergo a transition to the jth state with a probability equal to $k_{ij}(t)\Delta t$.

Throughout this paper, we use the following parameters: $\Gamma_d = \Gamma_a = k_{ex} = 1$ ns^{-1} and $f = 0.1$. These parameters are close to those for the FRET pair studied in ref 8. The kinetic Monte Carlo algorithm allows us to compute the second-order intensity correlation functions for fluorescence from the donor and the acceptor as defined by

$$g_{mn}(t' - t) = \frac{\langle I_m(t) I_n(t') \rangle}{\langle I_m \rangle \langle I_n \rangle} \tag{3}$$

where the subscripts $m =$ A, D and $n =$ A, D label the donor or the acceptor. Thus, we have three correlation functions, g_{AA}, g_{DD}, and g_{AD}, each of which can be measured experimentally.[8]

If photon emission events are temporally uncorrelated then one has $g_{mn} = 1$. For $m = n$, the quantity g_{nn} is an autocorrelation function. This quantity is above unit when the photons, emitted by the same source (either donor or acceptor), tend to arrive in "clusters" (bunching). It is below unit in the case of photon antibunching.

III. Results

In Figure 3, we plot the simulated signal, $g_{AA}(t)$, $g_{DD}(t)$, and $g_{AD}(t)$, for a pair of chromophores attached at the ends of a polypeptide chain that consists of 23 peptide units. The Förster radius is $R_0 = 20$ Å[31] and the diffusion coefficient $D = 3 \times 10^{-6}$ cm^2/s.[9,12−14] At short times, both $g_{AA}(t)$ and $g_{DD}(t)$ exhibit a "dip". This is the photon antibunching, a manifestation of the quantum nature of the emitted light. Once a chromophore emits a photon, it is in the ground state and therefore cannot emit a photon until it gets excited again. The dip in the cross-correlation function, $g_{AD}(t)$, has a different nature and is due to the diffusive dynamics of the polypeptide (such a dip is absent in the case where r is constant). Qualitatively, this is due to the fact that, depending on the interchromophore distance $r(t)$, when the donor emission I_D is strong then the acceptor emission I_A is weak and vice versa (see section IV). Thus, observation of photons emitted by the acceptor is negatively correlated with those from the donor.

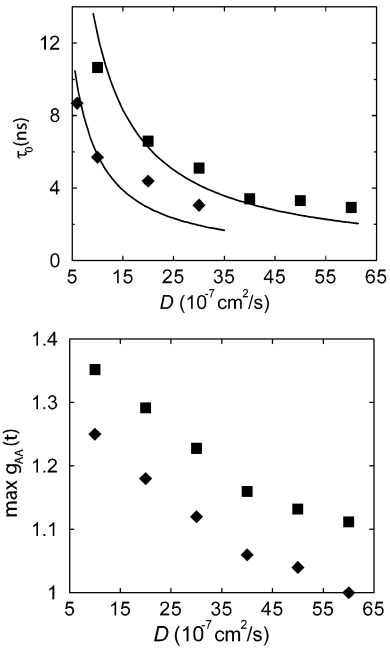

Figure 4. (a) τ_0 and (b) the peak value of $g_{AA}(t)$ as a function of the diffusion coefficient D for a chain that consists of 23 (squares) and 15 (diamonds) peptide units. The lines in Figure 4a are fits of the data using $\tau_0 \sim 1/D$. The Förster radius is $R_0 = 20$ Å.

The acceptor emission signal, $g_{AA}(t)$, also exhibits a maximum at longer times. This "bunching" signal is a signature of the diffusive dynamics of the peptide. It would be entirely absent if the FRET rate Γ_F were constant.

The decaying part of the signal is well described by an exponential function, $g_{AA}(t) \approx 1 + a_0 e^{-t/\tau_0}$. The two parameters, a_0 and τ_0, contain information about the statistics of the trajectories $r(t)$. Specifically, τ_0 is indicative of the time scale of the conformational dynamics. To probe these dynamics most accurately, it is desirable to maximize the magnitude of the bunching signal, which can be characterized by the peak values of $g_{AA}(t)$. Plotted in Figure 4 is the dependence of the time τ_0 (Figure 4a) and of the peak value of $g_{AA}(t)$ (Figure 4b) on the diffusion coefficient, for different values of R_0 and of the chain length. We find that the time τ_0 is inversely proportional to the diffusion coefficient D and that the magnitude of the bunching signal decreases as D is increased. If the molecule diffuses too fast, then the signal associated with the molecule's diffusion disappears. This sets an upper limit on the diffusion coefficient that can be measured in such an experiment: If, for instance, the lowest detectable signal corresponds to max $g_{AA}(t) > 1.2$ then the highest value of the diffusion coefficient that can be measured using the present FRET pair is about 4×10^{-6} cm^2/s for the $N = 23$ peptide and 2×10^{-6} cm^2/s for the $N = 15$ chain. The magnitude of the signal, max $g_{AA}(t)$, is higher for longer peptides.

We further plot the peak value of $g_{AA}(t)$ as a function of the Förster radius R_0 in Figure 5a. We find that there is an optimal value of R_0 that maximizes the observed signal. We will discuss the origins of this behavior in section IV.

In Figure 3, the intramolecular diffusion of the peptide has a pronounced effect on g_{AA}, while barely influencing the donor emission statistics. This is a consequence of the particular choice of the FRET parameters in our model. Specifically, the average FRET efficiency is low in our case. If the FRET efficiency is high, $g_{DD}(t)$ may also have a pronounced maximum. The physical reason for this behavior will be explained in Section IV.

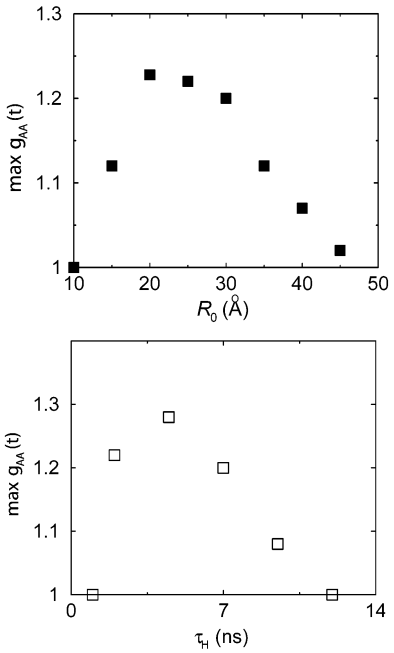

Figure 5. (a) Peak value of $g_{AA}(t)$ as a function of R_0. (b) The peak value of $g_{AA}(t)$ as a function of τ_H in the dual FRET model, in which the sum $\tau_H + \tau_L$ was kept constant (=14 ns). Other parameters of the model are $\Gamma_L = 0$, $\Gamma_H = 5$ ns^{-1}.

IV. Comparison with the Haas−Steinberg Theory

Haas and Steinberg[10] developed a theory for photon correlation statistics in a single molecule FRET experiment under the condition that the diffusive dynamics of the FRET pair is the slowest time scale in the problem. Specifically, the assumption is that the time scale for the fluctuations of $r(t)$ and therefore of $\Gamma_F(r(t))$ is much slower than $1/\Gamma_a$, $1/\Gamma_d$, and $1/\Gamma_F$. To obtain their result, we solve the kinetic equations (2) for the kinetic scheme in Figure 2b to find the steady-state population of each state, assuming that these populations adiabatically follow the slowly varying $\Gamma_F(t)$. For example, if the lifetimes of the donor and the acceptor are the same, $\Gamma_a = \Gamma_d = \Gamma$, then we find the probability that the donor alone is excited (i.e., the population of the state $|10\rangle$) to be

$$p_{10}(t) = p_{00}(t)\frac{k_{ex}}{\Gamma}\frac{2\Gamma + k_{ex}(1+f)}{2\Gamma + k_{ex}(1+f) + 2\Gamma_F(r(t))} \quad (4a)$$

where p_{00} is the population of the ground state. Similarly, the probability of exciting the acceptor alone, p_{01}, and the probability that both the donor and the acceptor are excited, p_{11}, are given by

$$p_{01}(t) = p_{00}(t)\frac{k_{ex}}{\Gamma}\frac{k_{ex}f(1+f) + 2\Gamma_F(r(t))(1+f) + 2f\Gamma}{2\Gamma + k_{ex}(1+f) + 2\Gamma_F(r(t))} \quad (4b)$$

$$p_{11}(t) = p_{00}(t)\left(\frac{k_{ex}}{\Gamma}\right)^2\frac{f^2k_{ex} + \Gamma_F(r(t)) + f(2\Gamma + k_{ex} + \Gamma_F(r(t)))}{2\Gamma + k_{ex}(1+f) + 2\Gamma_F(r(t))} \quad (4c)$$

These probabilities, of course, should add up to one, which determines the value of p_{00}. For the donor and the acceptor signal, we have

$$I_D(t) = \Gamma(p_{11}(t) + p_{10}(t))$$

$$I_A(t) = \Gamma(p_{11}(t) + p_{01}(t)) \quad (5)$$

In the limit $k_{ex}/\Gamma \ll 1$ implied in the Haas-Steinberg theory,[10] the equations become simpler

$$I_D(t) = \frac{k_{ex}}{1 + \Gamma_F(r(t))/\Gamma}$$

$$I_A(t) = k_{ex}\left(f + \frac{\Gamma_F(r(t))}{\Gamma_F(r(t)) + \Gamma}\right)$$

Then using eq 1, we find the correlation functions to be

$$g_{DD}(t'-t) = \langle I_D(t)I_D(t')\rangle/\langle I_D\rangle^2 = 1 + \frac{\langle\xi(t)\xi(t')\rangle - \langle\xi\rangle^2}{\langle\xi\rangle^2}$$

$$g_{AA}(t'-t) = \langle I_A(t)I_A(t')\rangle/\langle I_A\rangle^2 = 1 + \frac{\langle\xi(t)\xi(t')\rangle - \langle\xi\rangle^2}{(1+f-\langle\xi\rangle)^2}$$

$$g_{AD}(t'-t) = \frac{\langle I_A(t)I_D(t')\rangle}{\langle I_A\rangle\langle I_D\rangle} = 1 + \frac{\langle\xi\rangle^2 - \langle\xi(t)\xi(t')\rangle}{(1+f)\langle\xi\rangle - \langle\xi\rangle^2} \quad (6)$$

where the quantity

$$\xi(t) = \frac{r^6(t)}{R_0^6 + r^6(t)} \quad (7)$$

is related to the FRET efficiency $E(t) = 1 - \xi(t)$. The statistical properties of this quantity have previously been studied by Yang and co-workers[11] for semiflexible Gaussian chains.

By using $\xi(t)$ obtained from our Brownian dynamics simulation, we have computed the correlation functions g_{AA}, g_{DD}, and g_{AD} predicted by eq 6. The result is shown as dashed lines in Figure 3. In what follows, we point out some of the salient features of the photoemission statistics predicted by eq 6 and compare these predictions with our simulation data:

(i) Equation 6 predicts that in order to see a considerable signature of the diffusion in the signal g_{AA}, the Förster radius R_0 should be such that the acceptor emission rate I_A is weak; that is, the average FRET efficiency equal to $(1-\langle\xi\rangle)$ should be low. This requires that $\Gamma_F < \Gamma$ and that f is small. [More specifically, $g_{AA}(t)$ is larger than $g_{DD}(t)$ if $\langle\xi\rangle > (1+f)/2$]. Indeed, the absolute magnitude of the fluctuations in $I_A(t)$ and $I_D(t)$ is the same as the sum of the two, $I_A(t) + I_D(t) = k_{ex}(1+f)$, is constant. The magnitude of the signal, $g_{AA}(t)$ or $g_{DD}(t)$, is then controlled by the variation of the intensity *relative* to the average emission signal ($\langle I_A\rangle$ or $\langle I_D\rangle$). If the FRET efficiency is high then the relative fluctuations in I_A become small resulting in a weak signal. Similarly, the donor signal g_{DD} becomes pronounced when the FRET efficiency is high and I_D is low. This explains why in Figure 3 the autocorrelation function g_{DD} is weakly affected by the molecule's diffusion, as the chosen parameters of the FRET pair and of the peptide are such that the FRET efficiency is low.

(ii) According to eq 6, the functions $g_{DD}(t)$ and $g_{AA}(t)$ should exhibit a maximum at $t = 0$ as the correlation function $\langle\xi(0)\xi(t)\rangle$ does. The cross-correlation function $g_{AD}(t)$ however should exhibit a dip at short times because $\langle\xi(0)\xi(t)\rangle$ enters in the expression for $g_{AD}(t)$ with a minus sign. Physically, this dip results from the anticorrelation between I_A and I_D [i.e., whenever I_A is large, I_D is low and vice versa, so that the sum of these two intensities is constant, $I_A(t) + I_D(t) = k_{ex}(1+f)$]. These predictions are qualitatively (but not quantitatively) consistent with the simulation results shown in Figure 3 except for the fact that for short enough t (comparable with the excitation and

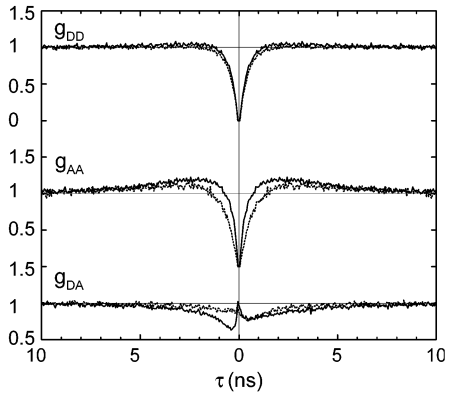

Figure 6. g_{AA}, g_{DD}, and g_{AD} calculated from the dual FRET model with $\tau_H = \tau_L = 7$ ns, $\Gamma_L = 0$ for $\Gamma_H = 5$ ns^{-1} (solid lines) and $\Gamma_H = 1$ ns^{-1} (dotted lines).

emission times) quantum effects dominate the observed signal, resulting in antibunching that, naturally, is not predicted by the classical theory described here. Equation 6 severely overestimates the bunching effect for $g_{AA}(t)$ for the same reason, as it neglects the competing effect from photon antibunching at short times.

(iii) From eq 6, in the limit $R_0 \rightarrow 0$, the function $\xi(t)$ is close to a constant value, $\xi(t) \approx 1$. Thus, eq 6 predicts that both g_{AA} and g_{DD} become equal to 1. The diffusive dynamics of the chain has no effect on the observed signal when the Förster radius is too short. In the limit $R_0 \rightarrow \infty$, the function $\xi(t)$ is proportional to R_0^{-6} so that $\xi(t) \ll 1$. We then find that the bunching effect vanishes in the correlation function g_{AA}. Therefore, we expect that the observed peak in $g_{AA}(t)$ should attain a maximum magnitude for some intermediate value of R_0, which generally depends on the chain length. This qualitative behavior is indeed observed in our simulation data as seen from Figure 5a. The behavior of $g_{DD}(t)$ in the limit $R_0 \rightarrow \infty$ is however different. The maximum in g_{DD} becomes independent of R_0 and does not disappear in this limit.

V. Comparison with the Dual FRET Model

Berglund and co-workers[8] introduced a dual FRET model in order to explain their experimental data for the signal from a FRET pair attached to a DNA molecule. As the dual FRET model shows behavior that is qualitatively similar to that observed in our simulations, we present here an analysis of this simpler model. It turns out that this analysis provides additional insight into the simulation results reported in section III.

In dual FRET model, it is assumed that the FRET rate $\Gamma_F(t)$ undergoes a stochastic process jumping between a higher value Γ_H and a lower one Γ_L. The probabilities p_H and p_L to have these values of the FRET rate satisfy the equations

$$dp_H/dt = -p_H/\tau_H + p_L/\tau_L$$
$$dp_L/dt = p_H/\tau_H - p_L/\tau_L \qquad (8)$$

where τ_L and τ_H are the mean residence times for the states with the high and low FRET rates. In Figure 6, we show the behavior of g_{AA}, g_{DD}, and g_{AD} for two values of Γ_H (5 and 1 ns^{-1}) with Γ_L equal to zero. There is a notable dependence on the FRET rate Γ_H: as it increases from 1 to 5 ns^{-1}, the acceptor bunching becomes more pronounced while the donor signal is barely changed. Further increasing Γ_H to 10 ns^{-1} does not significantly affect the signal. These features can be understood qualitatively by using the approximation described in section IV. According to this approximation, fluctuations in the FRET rate result in fluctuations in the acceptor emission signal $I_A(t)$, which undergoes a stochastic process jumping between two values, I_H and I_L. If, for example, $\tau_H = \tau_L = \tau$, then the acceptor intensity autocorrelation function can be calculated to be

$$g_{AA}(t) = 1 + \frac{(I_H - I_L)^2}{(I_H + I_L)^2} \exp(-2t/\tau) \qquad (9)$$

The intensities I_H and I_L can be calculated from eqs 4−5. According to eq 4, increasing Γ_H results in an increase in I_H thus leading to a more pronounced maximum in $g_{AA}(t)$. However, I_H saturates at higher values of Γ_H and becomes independent of the FRET rate for two reasons: First, the acceptor emission rate becomes limited by the emission rate Γ, and second, for high excitation rates k_{ex}, the FRET frequency by itself cannot increase indefinitely because it becomes limited by the fact that excitation cannot be transferred to the acceptor when the latter is excited. For the same reason, we observe that choosing a higher value of $\Gamma_L = 1$ ns^{-1} (and therefore a higher value of I_L) eliminates the bunching peak completely.

Other features seen in our FRET simulations can be readily understood from an analysis of the dual FRET model. For example, as seen in Figure 3, the asymptotic behavior of g_{AA} is well described by an exponential law $g_{AA}(t) \approx 1 + a_0 e^{-t/\tau_0}$ where τ_0 is proportional to the switching time $\tau_H = \tau_L$. Although in the simulations reported in section III the FRET rate is changing continuously, the characteristic time for altering the distance r (and therefore the FRET rate) is inversely proportional to the diffusion coefficient D. Thus, the two models show essentially the same behavior, in which the time scale of the asymptotic decay of the correlation function $g_{AA}(t)$ is related to the characteristic time scale for the conformational changes in the molecule.

Furthermore, we can understand the dependence of the observed signal on the Förster radius R_0 (Figure 5a) in the following way: We divide all of the peptide conformations into those with a high FRET rate (i.e., those with $r < R_0$) and those with a low FRET rate ($r > R_0$). Changing R_0 shifts the balance between the average times the peptide spends in the high- and low-Γ_F conformations. This effect or increasing R_0 while keeping D constant can be mimicked, in the dual-FRET model, by increasing τ_H while keeping the sum $\tau_H + \tau_L$ constant. Indeed, we find a nonmonotonic dependence of the peak value of g_{AA} on τ_H (see Figure 5b), which parallels the nonmonotonic R_0 dependence found for FRET in section III.

VI. Concluding Remarks

The behavior of the correlation functions g_{AA}, g_{DD}, and g_{AD} observed in our simulations is very similar to that observed for a pair of dye molecules on a DNA.[8] However, the physical origins of this behavior are quite different. Berglund et al. show that the assumption of "intermittent" FRET rates can explain the photoemission statistics in their experiment, whereas in our case, relative diffusion of the chain ends is responsible for the same features in the observed signal. The similarity between the results predicted by two different models (and in particular the lack of any nonexponential tails in the observed correlation functions) is to some extent discouraging because it suggests that, without independent insight into underlying physics of the system, the single molecule FRET cannot distinguish between alternative mechanisms. However, once the mechanism is established, our studies show that quantitative features of this mechanism can be extracted.

In the case where intramolecular diffusion is responsible for the observed features in the second order intensity correlation functions, we have seen that the diffusion coefficient is directly related to the time scale of decay of those correlation functions. The correlation functions g_{AA}, g_{DD}, and g_{AD} also contain information about the probability distribution $p(r)$ for the distance between the dye molecules. To illustrate this, ignore quantum effects and suppose that these correlation functions are well described by the classical theory of eqs 6 and 7. Then, from eq 6, we find

$$g_{DD}(0) = \langle \xi^2 \rangle / \langle \xi \rangle^2$$

$$g_{AA}(0) = 1 + \frac{\langle \xi^2 \rangle - \langle \xi \rangle^2}{(1 + f - \langle \xi \rangle)^2}$$

$$g_{AD}(0) = 1 + \frac{\langle \xi \rangle^2 - \langle \xi^2 \rangle}{(1 + f)\langle \xi \rangle - \langle \xi \rangle^2}$$

Therefore, measuring any two of these quantities will yield $\langle \xi \rangle$ and $\langle \xi^2 \rangle$, two moments of the probability distribution of the variable ξ and thus of the FRET efficiency $E = 1 - \xi$, which, in turn, is related to the probability distribution of the distance r. Naturally, this is not enough to recover the actual probability distribution of any of these quantities. However, if one has a reasonable physical model for the functional form of the distribution $p(r)$, then these moments may be sufficient to determine it. For example, in the case of random coil polymers, one could use the known scaling properties of $p(r)$ to parametrize this distribution.[32]

Acknowledgment. This work was supported by the Robert A. Welch foundation.

References and Notes

(1) Chan, B.; et al. Intra-tRNA distance measurements for nucleocapsid proteindependent tRNA unwinding during priming of HIV reverse transcription. *Proc. Natl. Acad. Sci. U.S.A.* **1999**, *96*, 459.

(2) Deniz, A. A.; et al. Single-molecule protein folding: Diffusion fluorescence resonance energy transfer studies of the denaturation of chymotrypsin inhibitor 2. *Proc. Natl. Acad. Sci. U.S.A.* **2000**, *97*, 5179.

(3) Jia, Y. et al. Folding dynamics of single GCN-4 peptides by fluorescence resonant energy transfer confocal microscopy. *Chem. Phys.* **1999**, *247*, 747.

(4) Schuler, B.; Lipman, E. A.; Eaton, W. A. Probing the free energy surface for protein folding with single-molecule fluorescence spectroscopy. *Nature* **2002**, *419*, 743.

(5) Talaga, D. S.; et al. Dynamics and folding of single two-stranded coiled-coil peptides studied by fluorescent energy transfer confocal microscopy. *Proc. Natl. Acad. Sci. U.S.A.* **2000**, *97* (24), 13021−13026.

(6) Weiss, S. *Science* **1999**, *283*, 1676.

(7) Weiss, S. Measuring conformational dynamics of biomolecules by single molecule fluorescence spectroscopy. *Nature Struct. Biol.* **2000**, *7* (9), 724.

(8) Berglund, A. J.; Doherty, A. C.; Mabuchi, H. Photon Statistics and Dynamics of Fluorescence Resonance Energy Transfer. *Phys. Rev. Lett.* **2002**, *89* (6), 068101−1.

(9) Eaton, W. A. et al. Fast kinetics and mechanisms in protein folding. *Annu. Rev. Biomol. Struct.* **2000**, *29*, 327−59.

(10) Haas, E.; Steinberg, I. Z. Intramolecular dynamics of chain molecules monitored by fluctuations in efficiency of excitation energy transfer. A theoretical study. *Biophys. J.* **1984**, *46*, 429.

(11) Yang, S.; Witkoskie, J. B.; Cao, J. Single molecule dynamics of semi-flexible Gaussian chains. *J. Chem. Phys.* **2003**, *117* (24), 11010.

(12) Wang, Z. S.; Makarov, D. E. Rate of intramolecular contact formation in peptides: The loop length dependence. *J. Chem. Phys.* **2002**, *117*, 4591.

(13) Thirumalai, D. Time scales for the formation of the most probable tertiary contacts in proteins with applications to cytochrome *c*. *J. Phys. Chem. B* **1999**, *103*, 608.

(14) Lapidus, L. J.; Eaton, W. A.; Hofrichter, J. Measuring the rate of intramolecular contact formation in polypeptides. *Proc. Natl. Acad. Sci. U.S.A.* **2000**, *97* (13), 7220.

(15) Jung, Y.; Barkai, E.; Silbey, R. J. A stochastic theory of single molecule spectroscopy. *Adv. Chem. Phys.* **2002**, *123*, 199.

(16) Jung, Y.; Barkai, E.; Silbey, R. J. Current status of single-molecule spectroscopy: Theoretical aspects. *J. Chem. Phys.* **2002**, *117*, 10980.

(17) Makarov, D. E.; Metiu, H. Control, with a rf field, of photon emission times by a single molecule and its connection to laser-induced localization of an electron in a double well. *J. Chem. Phys.* **2001**, *115* (13), 5989−5993.

(18) Makarov, D. E. Observation of single molecule transport at surfaces via scanning microscopies: Monte Carlo wave function study of a model problem. *Phys. Rev. E* **2002**, *65*, 051601.

(19) Makarov, D. E.; et al. On the interpretation of force extension curves of single protein molecules. *J. Chem. Phys.* **2002**, *116*, 7760.

(20) Haas, E.; Katchalski-Katzir, E.; Steinberg, I. Z. *Biopolymers* **1978**, *17*, 11−31.

(21) Szabo, A.; Schulten, K.; Schulten, Z. *J. Chem. Phys.* **1980**, *72*, 4350.

(22) Allen, M. P.; Tildesley, D. J. *Computer Simulation of Liquids*; Clarendon Press: Oxford, 1987.

(23) Hegerfeldt, G. C. *Phys. Rev. A* **1993**, *47*, 449.

(24) Carmichael, H. *An Open Systems Approach to Quantum Optics*; Springer: New York, 1993.

(25) Dalibard, J.; Castin, Y.; Molmer, K. *Phys. Rev. Lett.* **1992**, *68*, 580.

(26) Cohen-Tannoudji. In *Fundamental Systems in Quantum Optics*; Dalibard, J., Raimond, J. M., Zinn-Justin, J., Eds.; Elsevier: New York, 1992.

(27) Gardiner, C. W.; Parkins, A. S.; Zoller, P. *Phys. Rev. A* **1992**, *46*, 4363.

(28) Makarov, D. E.; Metiu, H. Quantum dynamics with dissipation: a treatment of dephasing in the stochastic Shroedinger equation. *J. Chem. Phys.* **1999**, *111* (22), 10126.

(29) Voter, A. F. Classically exact overlayer dynamics: Diffusion of rhodium clusters on Rh(100). *Phys. Rev. B* **1986**, *34*, 6819.

(30) Metiu, H.; Lu, Y. T.; Zhang, Z. Epitaxial growth and the art of computer simulations. *Science* **1992**, *255*, 1088.

(31) Wu, P.; Brand, L. Resonance energy transfer: methods and applications. *Anal. Biochem.* **1994**, *218*, 1.

(32) De Gennes, P. G. *Scaling concepts in polymer physics*; Cornell University Press: Ithaca, NY, 1979.